

ARTICLE

Scaling between structural relaxation and caged dynamics in $\text{Ca}_{0.4}\text{K}_{0.6}(\text{NO}_3)_{1.4}$ and glycerol: free volume, time scales and implications for the pressure-energy correlations

A. Ottochian and D. Leporini*

*Dipartimento di Fisica “Enrico Fermi”,
 Università di Pisa, Largo B. Pontecorvo 3, I-56127 Pisa, Italy*

(v4.4 released November 2008)

The scaling of the slow structural relaxation with the fast caged dynamics is evidenced in the molten salt $\text{Ca}_{0.4}\text{K}_{0.6}(\text{NO}_3)_{1.4}$ (CKN) over about thirteen decades of the structural relaxation time. Glycerol scaling was analyzed in detail. In glycerol, the short-time mean-square displacement $\langle u^2 \rangle$, a measure of the caged dynamics, is contributed by free-volume. It is seen that, in order to evidence the scaling, the observation time of the fast dynamics must be shorter than the time scales of the relaxation processes. Systems with both negligible (like CKN, glycerol and network glassformers) and high (like van der Waals liquids and polymers) pressure-energy correlations exhibit the scaling between the slow relaxation and the fast caged dynamics. According to the available experiments, an isomorph-invariant expression of the master curve of the scaled data is not distinguishable from a simpler not-invariant expression. Instead, the latter agrees better with the simulations on a wide class of model polymers.

Keywords: Glass Transition, Fast-dynamics, Relaxation

1. Introduction

Understanding the extraordinary viscous slow-down that accompanies glass formation is a major scientific challenge [1–3]. On approaching the glass transition (GT), trapping effects are more and more prominent. The average escape time from the cage of the first neighbors, i.e. the structural relaxation time τ_α , increases from a few picoseconds up to thousands of seconds. The rattling motion inside the cage occurs on picosecond time scales with amplitude $\langle u^2 \rangle^{1/2}$. This quantity is related to the Debye-Waller factor which, assuming harmonicity of thermal motion, takes the form $\exp(-q^2 \langle u^2 \rangle / 3)$ where q is the absolute value of the scattering vector. At first sight, due to the extreme time-scale separation between the rattling motion ($\sim 10^{-12}$ s) and the relaxation ($\tau_\alpha \sim 10^2$ s at GT), one expects the complete independence of the two motions. Nonetheless, several authors investigated their correlations, emphasizing in particular the link with the bulk elastic properties (for a review see ref. [4]). In this research field, the universal scaling between the structural relaxation time, or the shear viscosity, and $\langle u^2 \rangle$ was reported for several numerical models, including linear polymers, mixtures, prototypical glassformers like SiO_2 and o-terphenyl (OTP), and icosahedral glassformer [5–7]. The resulting master curve fits with the available experimental data from supercooled liquids, polymers and metallic glasses over about eighteen decades of relaxation times (or

*Corresponding author. Email: dino.leporini@df.unipi.it

viscosity in non-polymeric systems) and a very wide range of fragilities.

The present paper shows that the scaling between the structural relaxation time and $\langle u^2 \rangle$ also holds for the molten salt $\text{Ca}_{0.4}\text{K}_{0.6}(\text{NO}_3)_{1.4}$ (CKN) over about thirteen decades of τ_α . Glycerol scaling was analyzed in detail. The scaling of glycerol and, over a less wide range of relaxation times and viscosities, network glassformers like SiO_2 , GeO_2 and B_2O_3 was already reported [5–7]. Here, for the first time, the scaling of these systems and CKN will be discussed from the viewpoint of the pressure-energy correlations [8–10]. In addition, it is shown that the role of the free volume in glycerol is not negligible and that the scaling works only if the observation time of the fast dynamics is *shorter* than the time scales of the relaxation processes [7].

The paper first summarizes the results about the scaling between the structural relaxation and $\langle u^2 \rangle$. Then, the results on glycerol and CKN are discussed in detail. Finally, the conclusions are presented.

2. Scaling between viscous flow, structural relaxation and $\langle u^2 \rangle$

Fig.1 shows the scaling between the structural relaxation time τ_α and the viscosity η with respect to the reduced mean-square displacement (MSD), $\langle u^2 \rangle / \langle u_g^2 \rangle$, with $\langle u_g^2 \rangle = \langle u^2(T_g) \rangle$. The experimental data include supercooled liquids, polymers, metallic glasses over about eighteen decades of relaxation times and a very wide range of fragilities. The plot now includes the ionic liquid CKN as well. All the data in Fig.1 are at ambient pressure. The master curve of Fig.1 (black line) is expressed analytically by:

$$\log X = \alpha + \tilde{\beta} \frac{\langle u_g^2 \rangle}{\langle u^2 \rangle} + \tilde{\gamma} \left(\frac{\langle u_g^2 \rangle}{\langle u^2 \rangle} \right)^2 \quad (1)$$

with X equal to the reduced quantities τ_α/τ_0 or η/η_0 . The best-fit values ($\alpha = -0.424(1)$, $\tilde{\beta} = 1.62(6)$ and $\tilde{\gamma} = 12.3(1)$) were drawn by Molecular-Dynamics simulations (MD) on model polymeric systems [5] and mixtures, being confirmed by comparison with prototypical glassformers like SiO_2 and o-terphenyl, and icosahedral glassformer [6]. For the systems in Fig.1 Table 1 lists the MSD at the glass transition temperature, i.e. the temperature where $\tau_\alpha = 10^2$ s or $\eta = 10^{12}$ Pa · s, and the conversion factors τ_0 and η_0 between the actual time and viscosity units and the corresponding MD units, respectively. Note that the conversion factors are the *only* adjustable parameters of the overall scaling procedure. Table 1 shows also the (approximate) observation time of the fast dynamics by the experiments Δt . The structural relaxation times of the systems in Fig. 1 are comparable or longer than Δt . The Δt dependence of the scaling of glycerol is discussed in Sec. 5.

3. Scaling and the pressure-energy correlations

Fig.2 shows that, when the CKN structural relaxation time and the glycerol shear viscosity are plotted vs the reduced MSD, they collapse over about thirteen decades in a single master curve well described by Eq.1 within the error bars.

There is competition between van der Waals and Coulombic terms in the interacting potential of CKN and glycerol. This feature deserves consideration from the viewpoint of the pressure-energy correlations [8–10]. Such correlations are expected to be weak for CKN and glycerol, thus leading to the absence of isomorphic states

in these two systems [41]. Weak correlations are also expected for network glassformers like SiO_2 , GeO_2 and B_2O_3 which exhibit scaling (see Fig.1, not included in Fig.2 for clarity reasons) [5–7].

Strongly correlating systems, e.g. van der Waals liquids, have isomorphic states. Rigorously, any general theory of the liquid state must end up in relations expressed only in terms of isomorph invariants (constant quantities when evaluated over a set of isomorphic states) to deal with the strongly correlating systems (a criterion also known as the "isomorph filter" [10]). From this respect, the master curve given by Eq.1 with *constant* α, β, γ parameters does *not* pass the "isomorph filter" and then should be unable to encompass strongly correlating systems since:

$$\frac{\langle \tilde{u}_g^2 \rangle}{\langle \tilde{u}^2 \rangle} \neq \frac{\langle u_g^2 \rangle}{\langle u^2 \rangle} \quad , \quad \log \tilde{X} \neq \log X \quad (2)$$

where $\tilde{\zeta} \equiv \zeta/\zeta_0$ with ζ_0 equal to $\rho^{-1/3}$, $\rho^{-1/3}\sqrt{m/k_B T}$, $\rho^{2/3}\sqrt{mk_B T}$ for length, time and viscosity, respectively and $\tilde{X} = \tilde{\tau}_\alpha/\tilde{\tau}_0$, $\tilde{\eta}/\tilde{\eta}_0$ [41]. A proper isomorph-invariant modification of Eq.1 is:

$$\log \tilde{X} = C_1 + C_2 \frac{\langle \tilde{u}_g^2 \rangle}{\langle \tilde{u}^2 \rangle} + C_3 \left(\frac{\langle \tilde{u}_g^2 \rangle}{\langle \tilde{u}^2 \rangle} \right)^2 \quad (3)$$

where C_i , $i = 1, 2, 3$ are constants. The above equation is more complex in nature than Eq. 1 since it needs the density as additional input parameter.

The fact that Eq. 3 is constrained by the basic properties of strongly correlating systems, which are not accounted for by Eq. 1, poses the question of the flexibility of these master curves to deal with systems with either strong (like OTP, TNB or polymers) or weak (like CKN, glycerol and the network glassformers SiO_2 , GeO_2 and B_2O_3) pressure-energy correlations. May Eqs. 1 and 3 be discriminated? To date, little help is provided by the experiments. The experimental data plotted in Fig.1 are taken at ambient pressure by sweeping the temperature in a limited range, thus resulting in small density changes. Owing to the much larger changes of the structural relaxation time, the viscosity and MSD, the equalities $\log \tilde{X} \simeq \log X$, $\langle \tilde{u}_g^2 \rangle / \langle \tilde{u}^2 \rangle \simeq \langle u_g^2 \rangle / \langle u^2 \rangle$ hold to a good approximation and Eqs. 1, 3 are hardly distinguishable. To our knowledge, joint data concerning τ_α (or viscosity for non polymeric systems) and MSD from high-pressure experiments spanning larger density changes are not available yet. If no clear-cut conclusion on the experimental side may be still drawn, numerical studies offer more insight. In particular, Eqs. 1 and 3 were investigated in the temperature/density phase space of a class of model polymers with different chain lengths and generalized Lennard-Jones potentials having constant position and depth of their minimum [6]. Note that pressure-energy correlations change with the potential and the physical state [42]. The different systems were compared with no MSD or τ_α rescaling and Eq.1 was used as master curve by taking $\langle u_g^2 \rangle$ as a constant independent of the model polymer. These positions: i) rely on the finding that the raw curves τ_α vs $\langle u^2 \rangle$ for different systems superimpose very well, ii) fit in with the need to limit the number of adjustable parameters. To keep on an equal footing the comparison between the two master curves, an analogous position was adopted for Eq. 3, i.e. $\langle \tilde{u}_g^2 \rangle$ was set to a constant independent of the model polymer (a step still preserving the isomorph invariance of Eq.3). On this basis, Eq. 1 was found to be more consistent with the numerical data (see Fig.11 of ref. [6]). To summarize, if the experiments do not discriminate between the two versions of the master curve, the isomorph-invariant

version Eq. 3, which is more complex in nature than Eq. 1 as noted above, agrees less with the simulations of a wide class of polymeric systems.

4. Free volume effects in Glycerol

The closeness of $\langle u^2 \rangle$ with free-volume concepts was noted in experiments [43, 46–48], theories [4, 49, 50] and simulations [5, 6, 51] with some debate [52, 53]. The basic question is about the existence of some critical displacement above which structural changes take place and it was stated that the rearrangement only takes place when there is a local, temporary density decrease [4]. We refer also to previous experimental [54, 55], theoretical and simulation [56–59] work.

The ratio between the volume that is accessible to the monomer center-of-mass and the monomer volume is $v_0^{(MD)} \sim (2\langle u_g^2 \rangle^{1/2})^3$ in MD units [5, 6]. From our simulation data (first line of Table 1) one finds:

$$v_0^{(MD)} \sim 0.017 \quad (4)$$

Flory and coworkers proposed that the glass transition takes place under iso-free volume conditions with the universal value $v_0 \sim 0.025$ [60]. This supports the conclusion that $\langle u^2 \rangle$ and the free volume are related, as above noted.

To better elucidate the matter, we consider results from the Positron Annihilation Lifetime Spectroscopy (PALS) [43, 44, 46]. PALS is a structural technique to parametrize the free volume. In fact, the orthopositronium bound state of a positron has a strong tendency to localize in holes of low electron density and decays with lifetime τ_3 being related to the average cavity size. In particular, we test the ansatz :

$$\langle u^2 \rangle = C \tau_3 \quad (5)$$

where C is a constant. The above equation captures the essentials of the relation between τ_3 and $\langle u^2 \rangle$, both increasing with the free volume. Furthermore, it provides a simple procedure to compare PALS and $\langle u^2 \rangle$ data with no adjustable parameters. In fact, Eq.5 yields the equality $\langle u_g^2 \rangle / \langle u^2 \rangle = \tau_{3g} / \tau_3$, with $\tau_{3g} = \tau_3(T_g)$, i.e. the reduced MSD is equal to the reduced PALS lifetime τ_3 . In Fig. 3 the viscosity data of glycerol were plotted by replacing the reduced MSD with the reduced τ_3 and comparing the results to the master curve expressed by Eq. 1. The conversion factor between the actual and the MD viscosity units was adjusted to $\log \eta'_0 = \log \eta_0 - 1$. Other parameters like in Table 1. Fig. 3 shows that the scaling of the long-time dynamics by either the reduced τ_3 or the reduced MSD are quite close to each other over about ten decades in relaxation times, thus leading to the conclusion that $\langle u^2 \rangle$ and free-volume are correlated. Deviations are observed for glycerol when cage restructuring, and then the free-volume fluctuations, occurs on time scales shorter than the PALS observation time, i.e. $\tau_\alpha \lesssim \tau_3 \sim 2$ ns (see also ref.[44]). In this regime the cage dynamics still takes place (it is detectable for $\tau_\alpha \gtrsim 1 - 10$ ps) and $\langle u^2 \rangle$ is still well-defined [5, 6] but the observation time τ_3 is too long and almost temperature-independent [43].

It must be noted that PALS data are usually interpreted by a model assuming the spherical shape of the hole where the positron decays. The model relates τ_3 to the hole radius R [43]. In addition to Eq.5, we also tested the relation $\langle u^2 \rangle \propto R^\delta$ (R drawn by the fit of τ_3 data) and found that the correlation plot between $\log \eta$ and R^δ agrees with the master curve expressed by Eq. 1 with $\delta \sim 1$. However, being

a model-dependent conclusion involving adjustable parameters, we think that the analysis of the free-volume role in terms of Eq. 5 is more robust.

5. Time scales of $\langle u^2 \rangle$ in Glycerol

We now proceed and better clarify that the correct investigation of the cage rattling is ensured if the observation time of the fast dynamics is *shorter* than τ_α . Fig. 4 shows the correlation between $\langle u^2 \rangle$ and the viscosity data of glycerol. $\langle u^2 \rangle$ was taken as the mean square displacement within the time Δt , the latter depending on the energy resolution of the neutron scattering (NS) experiment. It is seen that the scaling between the long-time dynamics and $\langle u^2 \rangle_{\Delta t=0.4 \text{ ns}}$ is rather good even for $\tau_\alpha/\Delta t \sim 1$, whereas using $\langle u^2 \rangle_{\Delta t=5 \text{ ns}}$ leads to deviations from the universal master curve if $\tau_\alpha/\Delta t \lesssim 60$. This suggests that, if $\tau_\alpha \lesssim 300 \text{ ns}$, $\langle u^2 \rangle_{\Delta t=5 \text{ ns}}$ is contributed by components which are not related to the cage vibrational dynamics. One anticipates that these components have relaxational character. Interestingly, τ_3 from PALS tracks the universal master curve of the structural relaxation down to $\tau_\alpha \sim 3 \text{ ns}$ where $\tau_\alpha/\Delta t_{PALS} \sim \tau_\alpha/\tau_3 \sim 1$ (Fig.3). The finding seems to indicate that in the range $3 \text{ ns} \lesssim \tau_\alpha \lesssim 300 \text{ ns}$ the free-volume is less affected by the relaxation than MSD on the nanosecond time scale. The above discussion supports the conclusion that cage-rattling MSD must be measured on time scales Δt shorter than the time scales due to both the structural and the possible local relaxations. Shortening Δt results in a remarkable extension of the region where the scaling between the structural relaxation and the cage dynamics of glycerol is observed (Fig. 4). However, this effect is less apparent in OTP [7].

6. Conclusions

It is shown that one molten salt (CKN) and one hydrogen-bonded liquid (glycerol) exhibit the scaling between the mean-square displacement due to cage rattling, $\langle u^2 \rangle$, and the structural relaxation time or viscosity already observed in super-cooled liquids, polymers and metallic glasses. Systems with both negligible (like CKN, glycerol, SiO_2 , GeO_2 and B_2O_3) and high pressure-energy correlations (like OTP, TNB or polymers) exhibit the above scaling. According to the available experiments, an isomorph-invariant expression of the master curve of the scaled data is not distinguishable from a simpler not-invariant expression. Instead, the latter agrees better with the simulations of a wide class of model polymers. The cage rattling of glycerol is contributed by free-volume over about ten decades in relaxation times. Both PALS and neutron scattering experiments show that, in order to evidence the scaling, the observation time of the fast dynamics must be shorter than the time scales of the relaxation processes.

Acknowledgement

Discussions with J. Bartoš and K.L. Ngai are gratefully acknowledged.

References

- [1] C. Angell, *J. Non-Crystalline Sol.* 131-133 (1991) p.13–31.
- [2] C.A. Angell, *Science* 267 (1995) p.1924–1935.
- [3] P.G. Debenedetti and F.H. Stillinger, *Nature* 410 (2001) p.259–267.
- [4] J.C. Dyre, *Rev. Mod. Phys.* 78 (2006) p.953–972.
- [5] L. Larini, A. Ottochian, C. De Michele and D. Leporini, *Nature Physics* 4 (2008) p.42–45.
- [6] A. Ottochian, C. De Michele and D. Leporini, *J. Chem. Phys.* 131 (2009) p.224517.
- [7] A. Ottochian and D. Leporini, *J. Non-Cryst. Solids*, in press (2010).
- [8] N.P. Bailey, U.R. Pedersen, N. Gnan, T.B. Schröder and J.C. Dyre, *J. Chem. Phys.* 129 (2008) p.184507.
- [9] T.B. Schröder, N.P. Bailey, U.R. Pedersen, N. Gnan and J.C. Dyre, *J. Chem. Phys.* 131 (2009) p.234503.
- [10] N. Gnan, T.B. Schröder, U.R. Pedersen, N. Bailey and J.C. Dyre, *J. Chem. Phys.* 131 (2009) p.234504.
- [11] R.H. Doremus, *J. Appl. Phys.* 92 (2002) p.7619–7629.
- [12] A. Wischnewski, *PhD Thesis*, Heinrich-Heine Universität, Düsseldorf, 1998.
- [13] A. Sipp, Y. Bottinga and P. Richet, *J. Non-Cryst. Solids* 288 (2001) p.166 – 174.
- [14] S. Caponi, M. Zanatta, A. Fontana, L.E. Bove, L. Orsingher, F. Natali, C. Petrillo and F. Sacchetti, *Phys. Rev. B* 79 (2009), 172201 p.172201.
- [15] K.M. Bernatz, I. Echeverría, S.L. Simon and D.J. Plazek, *J. Non-Cryst. Solids* 289 (2001) p.9–16.
- [16] D. Engberg, A. Wischnewski, U. Buchenau, L. Börjesson, A.J. Dianoux, A.P. Sokolov and L.M. Torell, *Phys. Rev. B* 58 (1998) p.9087–9097.
- [17] D. Sidebottom, R. Bergman, L. Börjesson and L.M. Torell, *Phys. Rev. Lett.* 71 (1993) p.2260–2263.
- [18] R. Busch, E. Bakke and W.L. Johnson, *Acta Mater* 46 (1998) p.4725–4732.
- [19] A. Meyer, H. Franz, B. Sepiol, J. Wuttke and W. Petry, *Europhys. Lett.* 36 (1996) p.379–384.
- [20] H.Z. Cummins, J. Hernandez, W.M. Du and G. Li, *Phys. Rev. Lett.* 73 (1994) p.2935–2935.
- [21] J. Wuttke, W. Petry, G. Coddens and F. Fujara, *Phys. Rev. E* 52 (1995) p.4026–4034.
- [22] C.M. Roland, M.J. Schroeder, J.J. Fontanella and K.L. Ngai, *Macromolecules* 37 (2004) p.2630–2635.
- [23] B. Frick and L.J. Fetters, *Macromolecules* 27 (1994) p.974–980.
- [24] D.J. Plazek and J.H. Magill, *J. Chem. Phys.* 49 (1968) p.3678–3682.
- [25] K.L. Ngai, *J. Non-Cryst. Solids* 275 (2000) p.7 – 51.
- [26] H. Franz, W. Petry and A.Q.R. Baron, *Hyperfine Interact.* 123-124 (1999) p.865–879.
- [27] N. Menon, S.R. Nagel and D.C. Venerus, *Phys. Rev. Lett.* 73 (1994) p.963–966.
- [28] A. Tölle, *Rep. Prog. Phys.* 64 (2001) p.1473–1532.
- [29] U. Buchenau and R. Zorn, *Europhysics Letters* 18 (1992) p.523–529.
- [30] D.L. Sidebottom and C.M. Sorensen, *J. Chem. Phys.* 91 (1989) p.7153–7158.
- [31] E. Kartini, M.F. Collins, B. Collier, F. Mezei and E.C. Svensson, *Phys. Rev. B* 54 (1996) p.6292–6300.
- [32] K. Ngai and C. Roland, *Mat. Res. Soc. Symp. Proc* 455 (1997) p.81–90.
- [33] R. Zorn, *J. Phys.: Condens. Matter* 15 (2003) p.R1025–R1046.
- [34] B. Frick and D. Richter, *Science* 267 (1995) p.1939–1945.
- [35] B. Frick, D. Richter, W. Petry and U. Buchenau, *Z. Phys. B* 70 (1988) p.73–79.
- [36] C.M. Roland, K.L. Ngai, P.G. Santangelo, X. Qiu, M.D. Ediger and D.J. Plazek, *Macromolecules* 34 (2001) p.6159–6160.
- [37] T. Kanaya, K. Kaji, J. Bartos and M. Klimova, *Macromolecules* 30 (1997) p.1107–1110.
- [38] R.H. Colby, *Phys. Rev. E* 61 (2000) p.1783–1792.
- [39] C.L. Soles, J.F. Douglas, W.I. Wu and R.M. Dimeo, *Macromolecules* 36 (2003) p.373–379.
- [40] N.G. McCrum, B.E. Read and G. Williams *Anelastic and Dielectric Effects in Polymeric Solid*, Dover Publications, New York, 1991.
- [41] In a system with N particles and ρ density, two system states, say $(\mathbf{r}_1, \mathbf{r}_2, \dots, \mathbf{r}_N)$ and $(\mathbf{r}'_1, \mathbf{r}'_2, \dots, \mathbf{r}'_N)$, are isomorphic under the prescription that, if $\tilde{\mathbf{r}}_i = \tilde{\mathbf{r}}'_i$, $i = 1, \dots, N$ ($\tilde{\mathbf{r}}_i \equiv \rho^{1/3} \mathbf{r}_i$), then they have proportional configurational NVT Boltzmann factors [10].
- [42] D. Coslovich, C.M. Roland, *J. Chem. Phys.* 130, 014508 (2009).
- [43] K.L. Ngai, L.R. Bao, A.F. Yee and C.L. Soles, *Phys. Rev. Lett.* 87 (2001) p.215901.
- [44] J. Bartoš, O. Šauša, D. Račko, J. Kristiak and J. Fontanella, *J. Non-Cryst Solids* 351 (2005) p.2599–2604.
- [45] R. Busselez, R. Lefort, M. Guendouz, B. Frick, O. Merdignac-Conanec and D. Morineau, *J. Chem. Phys.* 130 (2009), 214502 p.214502.
- [46] T. Kanaya, T. Tsukushi, K. Kaji, J. Bartos and J. Kristiak, *Phys. Rev. E* 60 (1999) p.1906.
- [47] E. Duval, A. Mermet, N. Surovtsev, J. Jal and A. Dianoux, *Phil. Mag. B* 77 (1997) p.457.
- [48] E. Duval, A. Mermet, N. Surovtsev and A. Dianoux, *J. Non-Cryst Solids* 235-237 (1998) p.203.
- [49] R.W. Hall and P.G. Wolynes, *J. Chem. Phys.* 86 (1987) p.2943–2948.
- [50] K.L. Ngai, *Phil. Mag.* 84 (2004) p.1341–1353.
- [51] F.W. Starr, S. Sastry, J.F. Douglas and S.C. Glotzer, *Phys. Rev. Lett.* 89 (2002) p.125501.
- [52] A. Widmer-Cooper, H. Perry, P. Harrowell and D.R. Reichman, *Nature Physics* 4 (2008) p.711–715.
- [53] D.J. Ashton and J.P. Garrahan, *Eur. Phys. J. E* 30 (2009) p.303–307.
- [54] D. Prevosto, S. Capaccioli, M. Lucchesi, D. Leporini, P. Rolla, *J. Phys.: Condens. Matter* 16 (2004) 6597–6608.
- [55] A. Barbieri, G. Gorini, D. Leporini, *Phys. Rev. E* 69 (2004) 061509.
- [56] A. Barbieri, E. Campani, S. Capaccioli, D. Leporini, *J. Chem. Phys.* 120 (2004) 437–453.
- [57] A. Barbieri, D. Prevosto, M. Lucchesi, D. Leporini, *J. Phys.: Condens. Matter* 16 (2004) 6609–6618.
- [58] L. Alessi, L. Andreozzi, M. Faetti, D. Leporini, *J. Chem. Phys.* 114 (2001) 3631–3639.
- [59] C. De Michele, D. Leporini, *Phys. Rev. E* 63 (2001) 036701.
- [60] U.W. Gedde *Polymer Physics*, Chapman and Hall, London, London, 1995.

TABLES

Table 1.: Details about the systems in Fig.1 (arranged in order of increasing fragility) and the MD simulations used to derive Eq.1. The experimental structural relaxation time τ_α is drawn by dielectric spectroscopy apart from B_2O_3 and CKN. τ_0 and η_0 are the conversion factors between the actual time and viscosity units and the corresponding MD units, respectively. Note that, apart from B_2O_3 and CKN, $\log \tau_0$ and $\log \eta_0$ cover the narrow ranges $-1 > \log \tau_0 > -2$ and $-11 > \log \eta_0 > -12$. MSD is drawn by Incoherent Neutron Scattering (INS) or Mössbauer Spectroscopy (MS). The table lists the approximate observation time of the fast caged dynamics by the experiment Δt , the MSD at the glass transition $\langle u_g^2 \rangle$ (in Å^2) or, equivalently, the Lamb-Mössbauer factor $-\ln f_g$.

System	τ_α, η			MSD		
	quantity	$\log \tau_0, \log \eta_0$	ref.	technique (Δt)	$\langle u_g^2 \rangle, -\ln f_g$	ref.
MD	τ_α	0	[5, 6]	MD	0.01667	[5, 6]
SiO ₂	η	-2	[11]	INS (40ps)	0.081	[12]
GeO ₂	η	-1	[13]	INS (0.4ns)	0.191	[14]
B ₂ O ₃	η	+2.2	[15]	INS (40ps)	0.065	[16]
B ₂ O ₃	τ_α^\ddagger	-8.4	[17]	INS (40ps)	0.065	[16]
V4 [†] alloy	η	-1	[18]	MS (0.1 μ s)	0.885	[19]
Glycerol	η	-1	[20]	INS (0.4ns)	0.022	[21]
1,4 PI	τ_α	-12	[22]	INS (4ns)	0.427	[23]
TNB	η	-2	[24]	INS (0.4ns)	0.315	[25]
Fe+DBP	τ_α	-11	[26]	MS (0.1 μ s)	3.15	[26]
Fe+DBP	η	-2	[27]	MS (0.1 μ s)	3.05	[26]
OTP	τ_α	-11	[25]	INS (0.4ns)	0.215	[28]
OTP	η	-1	[28]	INS (0.4ns)	0.232	[28]
Selenium	η	-1.66	[29]	INS (20ps)	0.155	[29]
CKN	τ_α^\ddagger	-13.5	[30]	INS (10ps)	0.132	[31, 32]
1,4 PBD	τ_α	-11	[33]	INS (4ns)	0.102	[34, 35]
a-PP	τ_α	-11.5	[36]	INS (0.2ns)	0.13	[37]
PMMA	τ_α	-11.5	[38]	INS (5ns)	1.1	[39]
PVC	τ_α	-11	[40]	INS (5ns)	0.51	[39]

[†] Zr_{46.8}Ti_{8.2}Cu_{7.5}Ni₁₀Be_{27.5}

[‡] Data aggregated from different techniques.

Figure captions

Figure 1.: Reduced relaxation time and viscosity vs reduced MSD factor ($\langle u_g^2 \rangle = \langle u^2(T_g) \rangle$). The numbers in parenthesis denote the fragility m . The black curve is Eq.1. The colored curves bound the accuracy of Eq.1 [5, 6]. Refer to Table 1 for further details about the experiments.

Figure 2.: Reduced relaxation time (CKN) and viscosity (glycerol) vs the reduced MSD. The other curves have the same meaning of Fig. 1. The numbers in parenthesis denote the fragility m . Other parameters are listed in Table 1.

Figure 3.: Test of Eq. 5 for glycerol by using two different data sets for τ_3 , i.e. ref. [43] (Gly1) and ref.[44] (Gly2). The plots of the reduced glycerol viscosity vs. the reduced time τ_3/τ_{3g} ($\tau_{3g} = \tau_3(T_g)$) are compared with the master curve Eq.1 (black curve). The other curves have the same meaning of Fig. 1. τ_0 and η_0 are given in Table 1. $\log \eta'_0 = \log \eta_0 - 1$. Deviations are observed when the free-volume fluctuations become fast with respect to the PALS timescale, i.e. $\tau_\alpha \lesssim \tau_3 \sim 2$ ns.

Figure 4.: Reduced glycerol viscosity vs. the reduced MSD taken at two different timescales $\Delta t = h/\Delta E$ depending on the energy resolution of the neutron scattering experiment ΔE (IN13 and IN16 data from refs.[21] and [45], respectively). All the curves have the same meaning of Fig. 1. τ_0 and η_0 are given in Table 1. The arrows point to states with the indicated τ_α values.

Figures

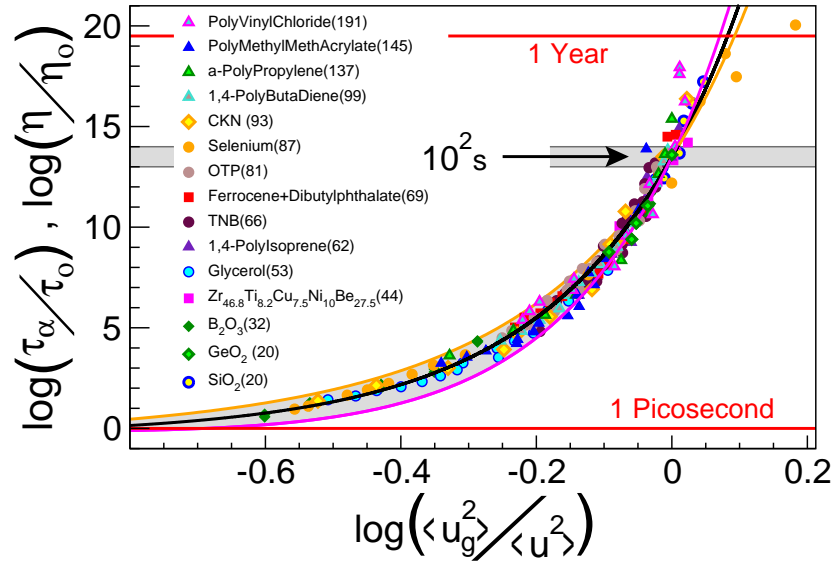


FIGURE 1

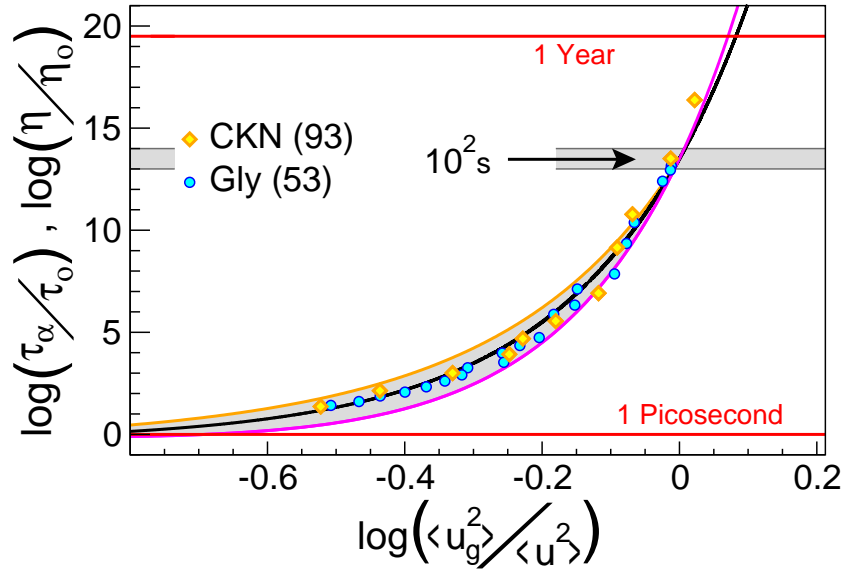


FIGURE 2

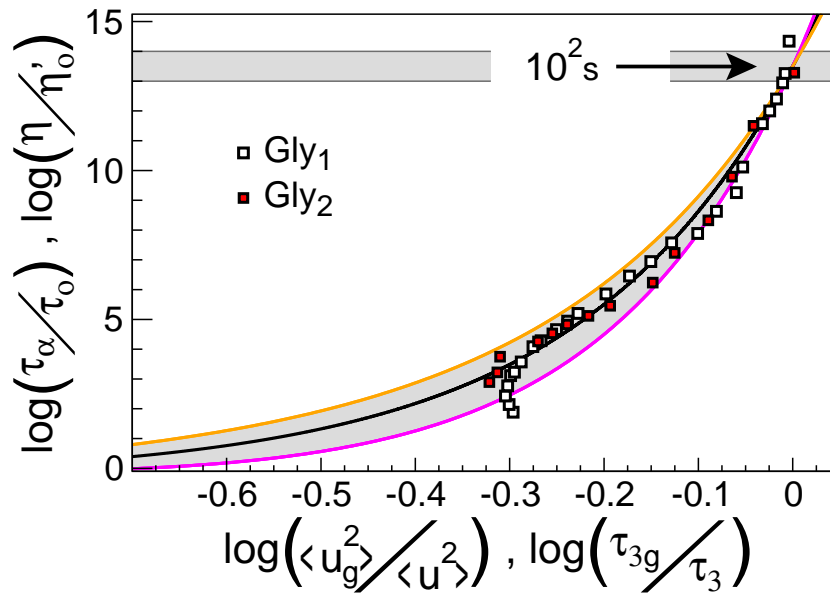


FIGURE 3

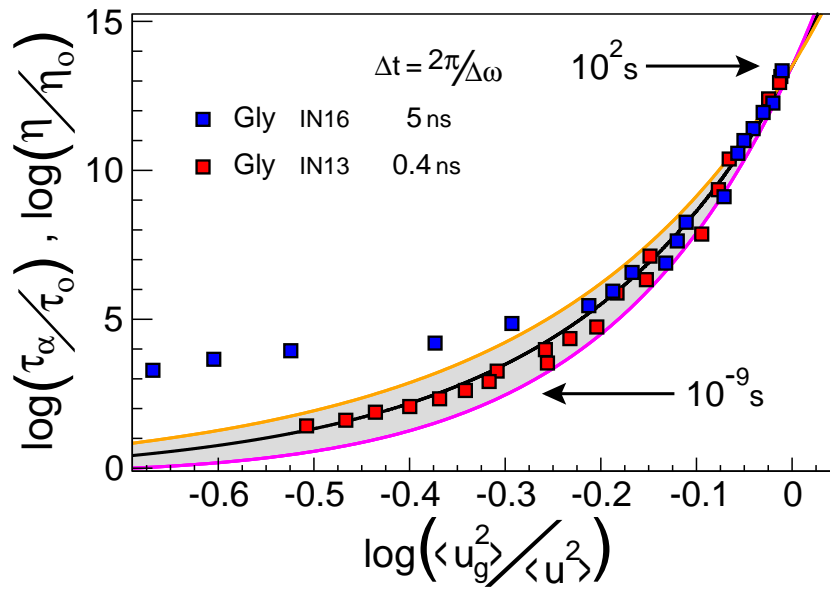


FIGURE 4